PRELIMINARY PERFORMANCE EVALUATIONS OF NON-IONIZING TERAHERTZ WOOD DENSITOMETRY

Caroline Marc(*), Bertrand Marcon, Louis Denaud, Stéphane Girardon, Jean-Claude Butaud
Arts et Metiers Institute of Technology, LABOMAP, HESAM Université, F-71250 Cluny, France
(*)*Email:* caroline.marc@ensam.eu

ABSTRACT

To use wood as a structural element in vehicles, it is necessary to measure its physical properties locally in order to deduce its mechanical behaviour. Density is one of the characteristics that influences the most the mechanical properties, and it is on its measurement that this study will focus, using a technology that is still little studied for this application: terahertz radiation. Measurements using a Terahertz radar on samples will allow to obtain maps of the optical index and absorption coefficient, these values being linked to the density of the samples. The present study will consider wood species with various global densities and exhibiting local density pattern (growth rings) to assess the prediction of the density.

Keywords: wood, mapping, terahertz waves, local density

INTRODUCTION

The wood mechanical and physical properties and its renewable character make it a material relevant to design structural elements in vehicles. However, its high intrinsic variability is not directly suited to the transport industry standards; hence the interest in measuring locally the wood physical properties, in order to be able to deduce its mechanical properties. Wood is a heterogeneous material. These density variations are present at different levels: annual growth rings, within the height and radius of the tree (decrease with height (Kord et al. 2010), and within the same species. These density variations are strongly correlated with the wood global mechanical properties (Guitard 1987). Other properties are also correlated with the local density such as the dimensional variations during drying or the thermal conduction.

In this study, terahertz frequency radiation spectroscopy will be used to measure density locally and without contact to obtain density maps among the whole veneer surface, using a Frequency Modulated Continuous Wave (FMCW) radar. The terahertz (THz) domain corresponds to electromagnetic waves comprised within the frequency range between 0.1 to 10 THz, and it suits the measurement of wood material for several reasons. Firstly, wood is semi-transparent to its rays unlike waves in the ultraviolet, visible and infrared range. Secondly, the energy of the photons associated with this frequency range is quite low, which is why THz radiation is non-ionizing, and therefore very little - if at all - harmful to health (Vander Vorst 2006), unlike X-rays for the same application. Finally, this wavelength allows to have a millimetric spatial resolution, that could be sufficient to measure density variations. However, it was not until the 1980s that these waves became commonly studied and then exploited, due to the lack of sufficiently powerful sources and detectors. Today, the emergence of new techniques and technologies makes terahertz a rapidly growing field of study (with more than 26,000 articles in 2021 compared to 10,400 in 2011 on Google Scholar with the keyword ‘Terahertz’). The

strong relationship between the absorption coefficient of wood at Terahertz frequencies and its density has already been demonstrated, using sources such as photoconductive antennas (Koch et al. 1998) or a Gunn diode (Chulkov et al. 2016), and the objective of this study is to test with an FMCW radar.

MATERIALS AND METHODS

Samples

Table 1 lists the main characteristics of the 7 samples studied in this study. A different combination of species and thickness is present in each sample, in order to observe the influence of these parameters on THz wave measurement. The species were selected to have a variety of wooden features, where Douglas Fir as a non-homogeneous softwood, and Beech as a homogeneous hardwood, Poplar is also a homogeneous hardwood, but the particularity of the sample is that it has two small dead knots (Figure 1). The samples were taken from a radial cut (LR cut, see Figure 1 below), which allows observing the density variations from earlywood to latewood.

Table 1 – Sample characteristics.

Name	Wood species	Thickness (mm)	Surface size (mm²)	MC (%)	Density (kg/m³)
D1	Douglas Fir	1	50×50	10.9	651
D3	Douglas Fir	3	50×50	10.0	588
D5	Douglas Fir	5	50×50	9.2	573
B1	Beech	1	50×50	10.9	744
B3	Beech	3	50×50	9.9	660
B5	Beech	5	50×50	9.0	685
P6	Poplar	6	50×50	10.5	371

A metallic tape serving as a perfect THz reflector will be placed on about a quarter of the back face of the samples for THz scanning. The waves having crossed the sample will be completely reflected by the tape, allowing to check if they have crossed all the thickness of the sample or not.

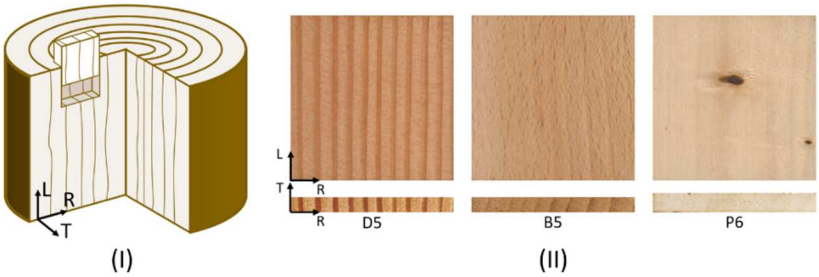

Fig. 1 – (I) Material wooden orientations within a tree and sample extraction example, (II) Pictures of a sample of each chosen species: Douglas Fir, Beech and Poplar (LR cut).

X-ray density measurement

The average density of each sample is known by weighing and measuring their external dimensions, but in order to be able to compare the THz wave measurements to density values at any point of the samples, the density was measured locally also using an X-rays imaging

system. The intensity transmitted through the sample I ($Sv.h^{-1}$) can be related to the density ρ ($g.cm^{-3}$) according to the Beer-Lambert law (equation 1), with μ the attenuation coefficient of the material ($cm^2.g^{-1}$), d the thickness of the sample (cm), and I_0 the intensity of the incident radiation ($Sv.h^{-1}$).

$$\rho = \frac{1}{\mu d}\log\left(\frac{I_0}{I}\right) \quad (1)$$

Assuming that the coefficient μ is the same for all samples and knowing that the levels of gray obtained following the measurement are proportional to the intensity of the wave transmitted, the relationship between gray level (GL) and density is written according to equation 2.

$$\rho \cdot d = a \cdot \ln(GL) + b \quad (2)$$

The values of parameters a and b are identified using pairs of values (gray level, $\rho \cdot d$) that are already known. The values of gray level and thickness are known at any point, assuming that the thickness is the same on the whole sample, while the average density for each sample is the only available information. A linear regression is therefore performed on the values of the product of the average density by the thickness according to the average of the logarithms of the gray levels per sample.

Frequency Modulated Continuous Wave terahertz radar

Measurements at THz frequencies were performed using a FMCW radar (Sub-THz FMCW Radar transceiver, Lytid). The operating of the FMCW radar measurement (Jankiraman 2018), illustrated in Figure 2 is the following: a signal is emitted by a voltage-controlled oscillator, with a progressively varying frequency due to a sawtooth modulation. This signal is multiplied in frequency and then transmitted to a target through the transmitting antenna. A portion of this signal is reflected back by the target, which corresponds to an interface between two media with different optical indices. The proportion of reflected signal depends, among other things, on the go through optical indices. The reflected signal is then received and combined with the emitted signal to produce the beating signal. The frequency of this signal (Δf in Figure 2) is proportional to the round-trip distance between the radar and the target.

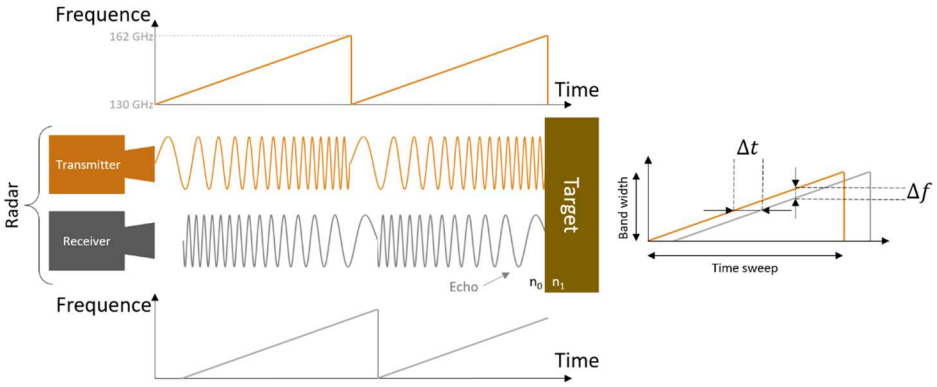

Fig, 2 – Operating principle of a FMCW radar.

If the signal encounters multiple targets on its path (e.g., irregularities in the sample or the backside of the sample), the beating signal can be decomposed into as many sinusoids as there are interfaces. Each sinusoid has a frequency related to the interface-radar distance. By analyzing the beat signal, information on the media with which the wave has interacted can be obtained, as well as the position of these media relative to the radar.

The equation 3 gives the relation between the beating signal frequency (Δf) and the distance to the target (z):

$$z = \frac{c \times \Delta t}{2n} = \frac{c \times \Delta f \times T_s}{2n \times BW} \quad (3)$$

with c the speed of light (m.s^{-1}), Δt the time delay between emitted and received signal (s), n the optical index of the propagation medium (-), Ts the sweep time (65 µs) and BW the sweep bandwidth (32 GHz).

Before the samples are measured, the radar must be calibrated: first, a measurement is performed on the background, and then a measurement is performed on a reference, which is a metallic mirror placed in the plane of the waist sensing point of the optical setup. This enables some noise related to optics to be filtered out, and the plane of the mirror is set as the reference plane, i.e. the zero beating frequency. Afterwards, the samples are positioned on the displacement plates to scan all their surfaces with a resolution of 1 mm², with their first face positioned at the level of the reference plane.

Preliminary radar data processing

The data obtained from the radar scans of the samples consist of temporal signals, with one signal acquired every 1 mm². To process these data, some preliminary quite usual signal treatments must first be done, and in particular to place oneself in the frequency domain, to be able to focus on the frequency range that concerns the interactions with the sample. To begin with, a Hamming window function is applied to the signal in order to damp its extremities towards 0 in order to perform a zero-padding (Bergounioux 2014). This operation is used to improve the longitudinal resolution (tangential direction of the wood) in distance. Indeed, the sampling frequency is Fs = 15.6 MHz, which allows obtaining 1024 values per signal. Thus, after going into the frequency domain, the frequency resolution is obtained by dividing Fs by 1024, which corresponds according to equation 3 to a distance resolution of 4.7 mm and to a distance of the order of magnitude of the thickest wood samples. The zero-padding allows the artificially increasing of this resolution by adding zeros at the end of the temporal signal, which increases the number of samples, while keeping the same frequency band (Fs) and without adding information. A zero-padding factor of 64 is used here, which gives a frequency resolution of Fs divided by 1024×64, corresponding to a frequency resolution of 238.4 Hz and to 0.07 mm in distance, thus much more consistent with the dimensions of the measured elements. After the zero-padding, the signal is subjected to a Fourier transformation, then finally it is normalized by dividing it by the maximum of the absolute value of an array composed of 1 of size 64×1024 having undergone the same operations as the signal (windowing, zero-padding then FFT). The normalized signal thus obtained corresponds to the ratio of the received signal to the transmitted signal.

Extraction of the parameters of the crossed environment

The beating signal contains information about the media that the radar wave has crossed. Among this information, the parameters that will be studied to determine their relationship with density are the optical index n and the absorption coefficient α (m^{-1}). To calculate these two parameters at all points of the samples (1 mm² resolution), the methodology used here will be to model the beating signal as a function of n and α, and then find the pair of values of n and α that produce the theoretical signal that is most similar to the experimental signal. In this study, two assumptions have been made to simplify the modeling. The first assumption is that the

samples are uniform in the transverse direction, meaning that n, α, and ρ are constant across the sample thickness. The second assumption is that the light-matter interactions such as refraction, scattering, and diffraction are negligible in the studied case and therefore not considered in the modeling, unlike reflection and attenuation.

Signal modeling

The formula for the beating signal is written according to equation 4 (Chopard 2021), where p represents the number of interfaces, r_i is the amplitude coefficient, τ_i is the time of flight, and Δf_{min} is the first frequency emitted during the sweep (130 GHz). As shown in Figure 3, it will be considered that $p = 3$, with the first two interfaces representing the front and back sides of the sample, and the third interface representing the back side once the wave has completed a round trip through the sample.

$$S_b(t) = \sum_{i=1}^{p} r_i e^{j2\pi\left(\Delta f_{min}\tau_i + \frac{BW}{T_s}\tau_i t\right)} \tag{4}$$

The values of τ_i and r_i are determined using equations 5 and 6, respectively. The amplitude coefficients of the beating signals correspond to those of the reflected signals at the three interfaces, namely S_r(t), S_{trt}(t) and S_{trrrt}(t) shown in Figure 3.

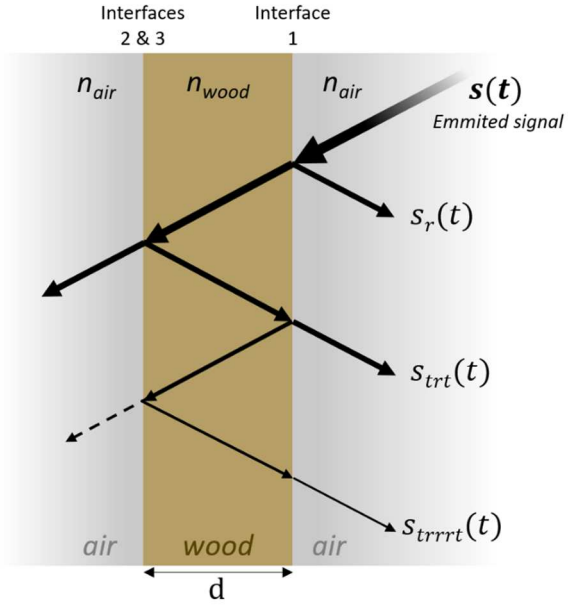

Fig. 3 – Signal path diagram.

These coefficients are calculated using formulas that consider the Fresnel coefficients for reflection (r_{i_j}) and transmission (t_{i_j}) explained in equations 7 and 8, respectively. Additionally, the influence of absorption is considered based on the Beer-Lambert law (equation 1).

$$\begin{aligned} \tau_1 &= 0 \\ \tau_2 &= 2 \times d \times n_{wood}/c \\ \tau_3 &= 4 \times d \times n_{wood}/c \end{aligned} \tag{5}$$

$$\begin{aligned} r_1 &= r_{air_{wood}} \\ r_2 &= t^2_{air_{wood}} \times r_{wood_{air}} \times e^{-2\alpha d} \\ r_3 &= t^2_{air_{wood}} \times r^3_{wood_{air}} \times e^{-4\alpha d} \end{aligned} \tag{6}$$

The theoretical signal is generated using the same sampling frequency as the experimental signal, then the preliminary processing detailed in the subsection 2.4 is applied to it. Finally, the modelled depends on 3 variables: the sample thickness d, which is known, the optical index n and the absorption coefficient α.

Optical index and absorption coefficient determination

As previously mentioned, the n and α of the medium can be determined by comparing the theoretical and experimental signals. To achieve this, the function described in equation 9, being the root mean square error (RMSE) between the amplitude of the two signals (with n and α as parameters), is then minimized to approach the theoretical model to the experimental signal as much as possible considering the initial simplifications enumerated before avoiding the perfect correspondence but still exhibiting great agreements.

The observed signal is not observed in its entirety, and a sample size T of 200 is taken, which corresponds to the first 200 samples starting from the zero-beating frequency. This sample size corresponds to a 14 mm distance, which includes the part of the signal reflected at the first interface as well as the part reflected at the third interface, even for the thickest samples.

$$RMSE(n,\alpha) = \sqrt{\frac{\sum_{t=1}^{T}\left(|S_b(n,\alpha)|_t - |S_{b\_exp}|_t\right)^2}{T}} \quad (9)$$

Spatial alignment between X-ray and THz scans

Both X-ray and THz radar methods provide 1 mm² spatial resolution maps. However, due to the samples being held in jaws during the scans, two edges are not visible on the maps. As a result, it can be challenging to accurately locate the samples and align the two types of maps. To overcome this challenge, the profiles of the data averaged along the longitudinal direction are realigned with each other for each sample, as shown in Figure 4.

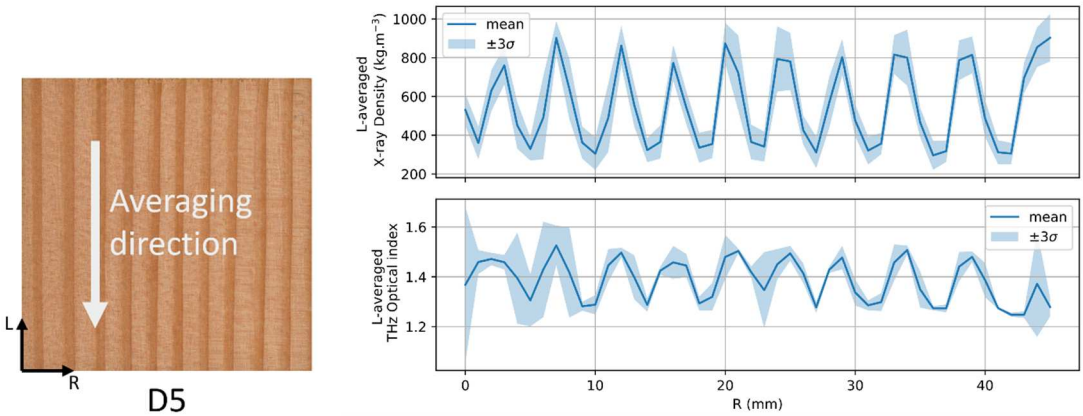

Fig. 4 – Density and optical index profile of the 5 mm thick Douglas Fir sample.

RESULTS AND DISCUSSION

Result of the modelling

Figure 5 displays density maps obtained by X-rays and the modeling results of the beating signals from the THz radar measurement for each sample.

The density maps reveal density variations linked to growth rings and the presence of knots. However, the maps of thinner samples show more visible noise than those of thicker samples.

Regarding the maps obtained from THz data, including optical index, absorption coefficient, and RMSE, the first observation is that the metallic tape placed at the back of the samples is visible in all of them, indicating that the wave makes at least one round trip in the material. Additionally, the model on samples B1 and B3 appears to be less successful than on the other samples. This is evidenced by the growth rings being less discernible or not visible at all in the case of B1. The elongated spots on the y-axis of the optical index and absorption coefficient mappings of sample B3 correspond to large rays visible on the surface of the sample.

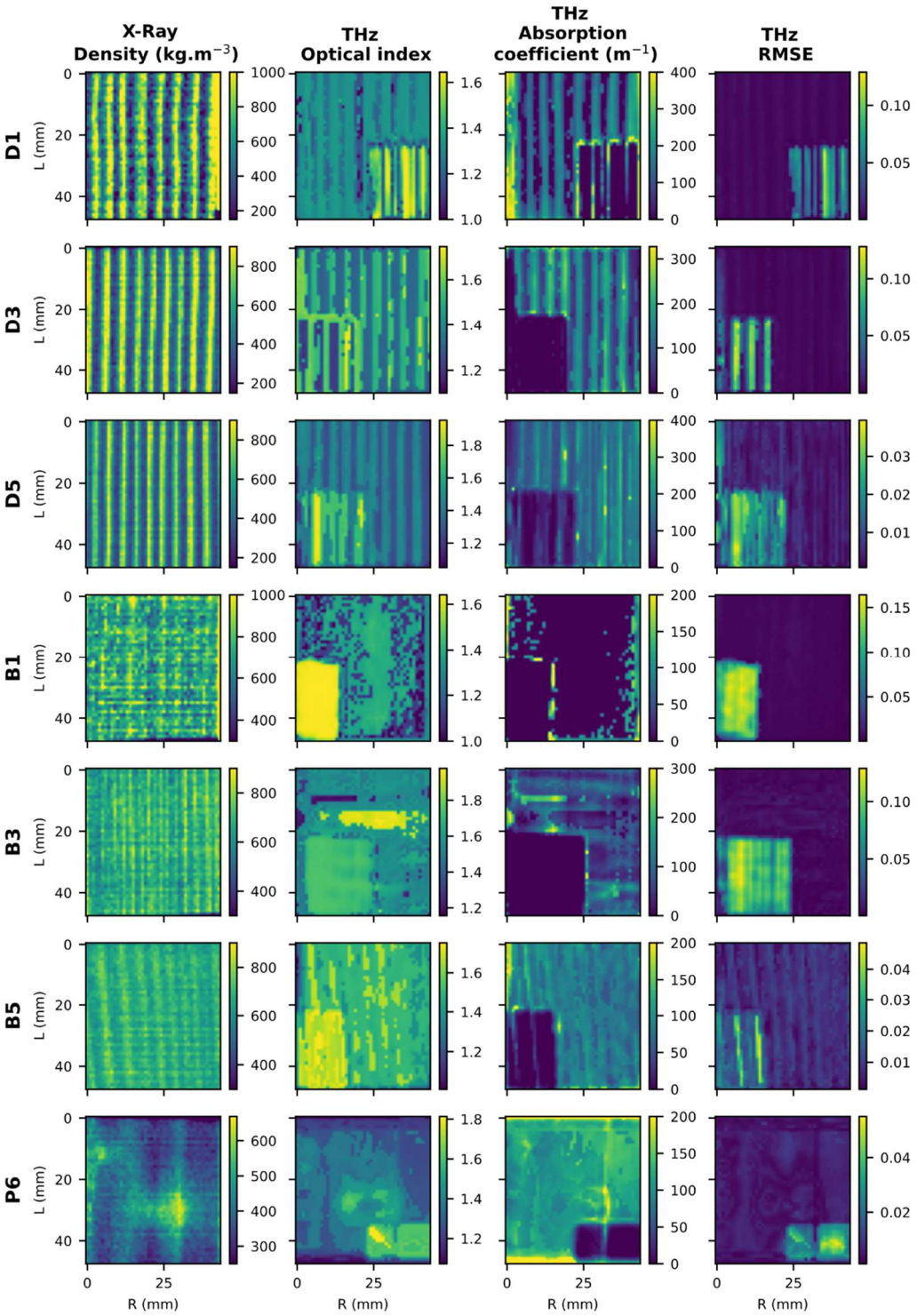

Fig. 5 – Density, optical index, absorption coefficient and RMSE maps of each sample.

Comparison between density and optical index maps

Figure 5 reveals a discernible relationship between density and the results of THz beating signal modeling. To further investigate this relationship, Figure 6 plots the optical index versus the density maps, where each point on the scatter plot corresponds to a pixel of the scan performed.

The analysis focuses on the points with RMSE values lower than a threshold, set to the sum of the mean of the RMSE and its standard deviation. This criterion is used to exclude points on the metallic tape and those with the least optimal modelling.

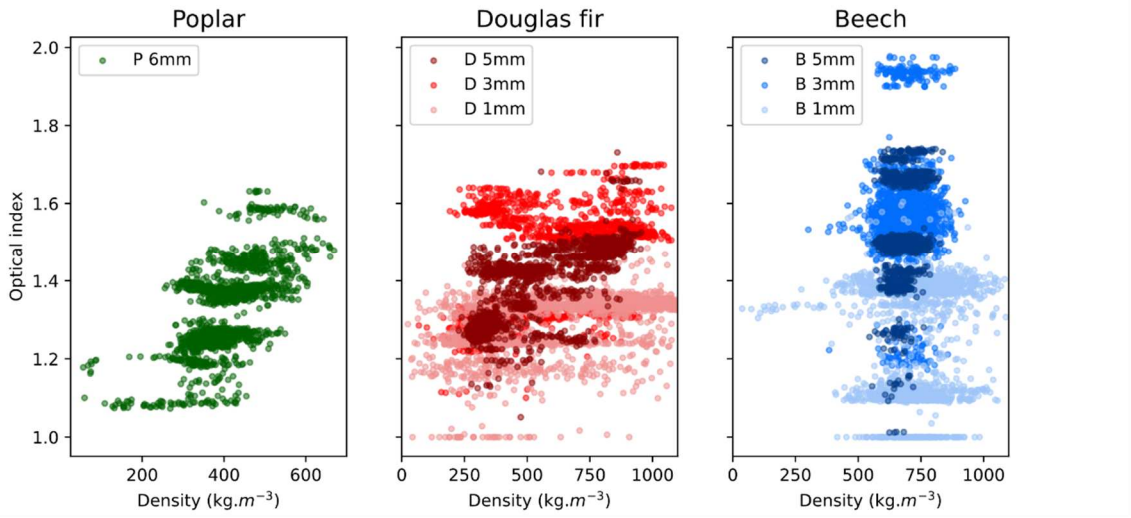

Fig. 6 – Scatter plot of optical index versus density for each species.

Table 2 presents the coefficients of determination (R^2) and p-values obtained from the linear regression of each scatter plot. Thicker samples show better correlation, which may be due to the thickness of the samples being too close to the wavelength of the emitted signal, which is about 2 mm. Indeed, the radar may have difficulty discerning the effects of each interface when they are separated by a distance less than or similar to the wavelength. For the Douglas Fir and poplar samples, the p-value is well below 1%, indicating a strong presumption against the hypothesis that there is no relationship between density and optical index. Sample B5 has a much lower R^2 than these samples, but its p-value is also well below 1%. However, the results of the linear regression do not allow us to make a statement about the optical index-density relationship for the others beech samples.

Table 2 – Results of the linear regression between THz and RX data.

Sample	Regression between the optical index and the density		Regression between the absorption coefficient and the density	
	R²	p-value	R²	p-value
D1	16.0%	<<0.01	10.7%	<<0.01
D3	26.4%	<<0.01	16.0%	<<0.01
D5	52.6%	<<0.01	13.9%	<<0.01
B1	0.0%	0.4	0.2%	0.1
B3	0.0%	0.2	0.0%	0.4
B5	6.8%	<<0.01	0.8%	<<0.01
P6	35.8%	<<0.01	13.6%	<<0.01

Comparison between density and absportion coefficient maps

Figure 7 and the right side of Table 2 pertain to the comparison between density and absorption coefficient, with data filtered using the RMSE. Upon examination, many points on the scatter plot of the Douglas Fir and beech samples have an absorption coefficient of zero, which is unrealistic since it would imply that the intensity of the wave did not decrease after passing through the sample. This indicates a problem with the modeling, since the RMSE appears to be satisfactory. Other than these anomalies, the conclusion drawn is largely consistent with the comparison between density and optical index concerning the p-value, with a lower R^2.

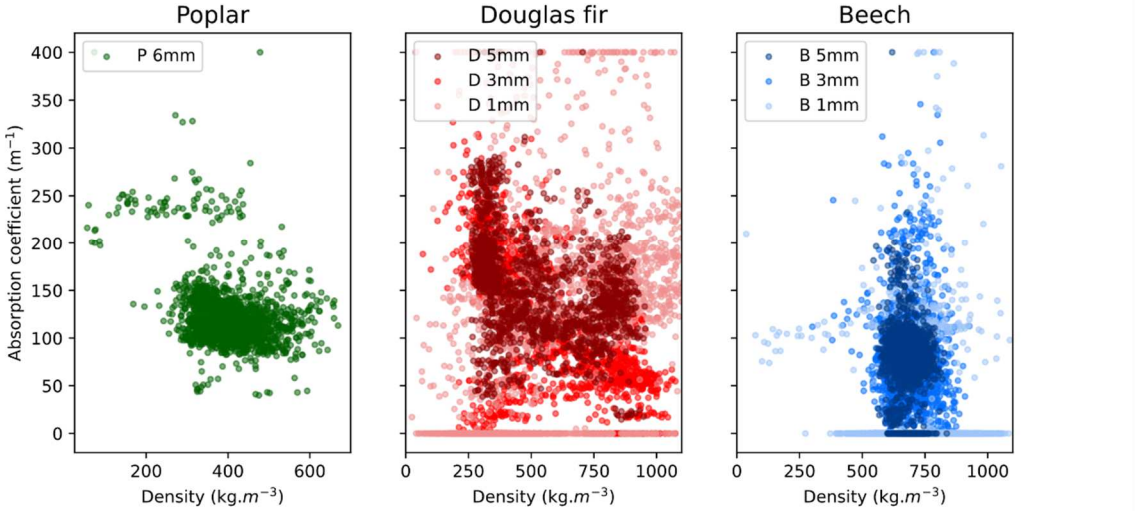

Fig. 7 – Scatter plot of absorption coefficient versus density for each species.

Discussion

In conclusion, these tests do not provide a quantitative relationship between the THz radar measurements and density, but they do show a clear correlation between the two. There are several reasons for the lack of precision. First, the assumptions made in the initial modeling may not hold in all cases, as visible in sample B5 where the assumption that n, α, and ρ are constant in thickness is clearly not applicable (see Figure 1- II). Second, the slight noise observed in the density maps likely hinders improvements to the correlations. Additionally, the sample and growth ring thicknesses are too small compared to the THz wavelength and the about 2 mm diameter of the spot. When the spot is positioned over a passage between earlywood and latewood, it is possible for the wave to split into two parts, each crossing media with different properties that are not accounted for in the modeling. Finally, improving the XY shift accuracy could also improve the correlations.

CONCLUSION

To the best of authors' knowledge, this is the first study to deal with densitometric measurement of wood using FMCW radar at terahertz frequencies. This was achieved by extracting the characteristics of the mediums through which the radar signals pass, and comparing them to a control density measurement made with an X-ray scanner.

However, due to numerous factors such as the simplistic signal modeling and unsuitable samples, accurate density information could not be extracted from the terahertz radar

measurements by comparison with the control measurement. Nevertheless, the results of the correlations between the two measurement methods demonstrate a relationship, with most p-values being lower than 1%.

These promising findings indicate the potential for non-ionizing densitometric measurement of wood using terahertz radar, and further investigation taking into account the difficulties encountered in this study will be conducted in future research.

ACKNOWLEDGMENTS

This PhD thesis is funded under the ANR-21-CE43-0008-02 project. The authors also thank the technical platform Xylomat of the scientific network Xylomat financed by the ANR-10-EQPX-16 XYLOFOREST which was largely used to carry out this study.

REFERENCES

[1] Bergounioux Maïtine 2014, Mathématiques pour le traitement du signal. Dunod.

[2] Chopard Adrien 2021, Terahertz Inspection Through FMCW Radar Developments and Advanced Imaging Approaches. École doctorale des sciences physiques et de l'ingénieur. https://www.theses.fr/2021BORD0315.

[3] Chulkov AO et al. 2016, Estimating the Humidity of Wood by Terahertz Infrared Thermography, Russian Journal of Nondestructive Testing 52(12): pp.753-57.

[4] Jankiraman M 2018, FMCW Radar Design. Artech House.

[5] Koch M et al. 1998, THz-Imaging: A New Method for Density Mapping of Wood. Wood Science and Technology: 7.